

Document downloaded from:

<http://hdl.handle.net/10251/103227>

This paper must be cited as:

Medina, JR.; Aguilar Herrando, J.; Diez, JJ. (1985). Distortions associated with random sea simulators. *Journal of Waterway Port Coastal and Ocean Engineering*. 111(4):603-627.
doi:10.1061/(ASCE)0733-950X(1985)111:4(603)



The final publication is available at

[http://doi.org/10.1061/\(ASCE\)0733-950X\(1985\)111:4\(603\)](http://doi.org/10.1061/(ASCE)0733-950X(1985)111:4(603))

Copyright American Society of Civil Engineers

Additional Information

DISTORTIONS ASSOCIATED WITH RANDOM SEA SIMULATORS

KEY WORDS : Algorithms; Computer simulation; Fourier transformation; Mathematical models; Stochastic processes; Water waves

ABSTRACT : Some numerical techniques for simulating Gaussian ergodic stochastic sea models are described, analyzed and contrasted. A general method for generating all numerical, linear, one-dimensional simulators by wave superposition permits one to describe or create any of these numerical random sea simulators in five steps. The distortions associated with each numerical simulator by wave superposition are analyzed from a general point of view and the arbitrariness of some numerical simulation techniques commonly used is noted. The time-consumed in ^{these} Monte Carlo experiments is an important factor. The numerical algorithms used can change indirectly the level of distortions associated with each numerical simulation technique. A special reference has been made to the use of the fast Fourier transform (FFT) for computing and to the second-order autoregressive behaviour of each wave component in order to reduce the time-consumed. Three criteria are proposed for qualifying the numerical simulators in order to adapt the requirements of each numerical experiment considered. To explain the variability of random sea, the deterministic amplitude component simulators are rejected while a nondeterministic spectral amplitude simulator (NSA) using a FFT algorithm can be employed.

SUMMARY : Numerical simulation techniques for linear random sea models are analyzed resulting in a general method to generate all wave superposition simulators, the distortions associated with them and the role of the efficient algorithms for computing these Monte Carlo experiments.

DISTORTIONS ASSOCIATED WITH RANDOM SEA SIMULATORS

By Josep R. Medina¹, José Aguilar², and J. Javier Diez³

INTRODUCTION

The numerical random sea simulation techniques of stationary stochastic processes defined by their continuous variance spectrum and the results obtained in the numerical experiments involved are illustrated in numerous coastal and ocean engineering publications. These Monte Carlo methods are especially significant for random sea simulations in which the spectral description of the sea surface has long been used. Kinsman(25) focuses on the sea spectral description history from an oceanographic point of view. He mentions the Gaussian(linear), ergodic (stationary) stochastic model first and later alludes to nonlinear models developed by Hasselman(18,19,20), Longuet-Higgins(27,28), and other researchers. On the other hand, directional sea models have been developed and this has signified an added degree of complication with respect to the linear, ergodic, one-dimensional model.

Various random sea models have been used in several different numerical experiments to solve distinct problems: Hudspeth and Min-Chu-Chen(23) utilized a stationary, one-dimensional, nonlinear stochastic model to carry ^{cut} on a dynamic analysis of multilegged pile-supported ocean structures; Goda(13) employed a stationary, directional, linear stochastic model to study directional wave register systems; Hudspeth and Borgman(22) used a stationary, one-dimensional linear version for generating efficient large random surface gravity waves by a hinged wavemaker, and other numerical simulation models for the study of a wide range of coastal and oceanic engineering problems.

¹Asst. Prof., Dept. of Ports and Ocean. Engrg., E.T.S. Caminos, Universidad
Politécnica de Valencia, Spain.

²Asst. Prof., Dept. of Ports and Ocean. Engrg., E.T.S. Caminos, U.P.V., Spain.

³Prof. of Ports and Ocean. Engrg., E.T.S. Caminos, U.P.V., Spain.

Although it can be stated that a real wave field ^{may} could be considered a nonstationary directional nonlinear stochastic process, the limited volume of real wave data available justifies simplified models for describing random seas. It can be said that all available numerical random sea models are theoretically incorrect, but they are in some sense justified; perhaps for this reason some recent publications such as the study of wave grouping by Goda(12) or the comparison of numerical random sea simulations by Tuah and Hudspeth(36) use different simulation techniques without any unifying criterion to get the best simulation technique for each specific case.

The simulation techniques for ocean engineering applications presented by Borgman(2) pointed out the two basic methods for linear random ocean wave simulators: the filtering of white noise by a determined digital linear system and the wave superposition method. Goda(13) explains the advantages of the latter method for numerical experiments while Houm and Overvik(21) assume the digital filtering techniques for generating waves in model flumes. Tuah and Hudspeth(36) carry out the numerical simulations by nondeterministic spectral amplitude(NSA) and deterministic spectral amplitude(DSA) models using a fast Fourier transform (FFT) algorithm to simulate stationary linear random wave realizations employing the process of filtering Gaussian white noise in the frequency domain. It will be shown that these techniques are especial algorithms for efficient simulation within the wave superposition method.

This paper proposes the establishment of a general structure and a unified criterion for the discussion of the best numerical simulation technique for each problem. The study is centered on stationary linear stochastic models which are the bases for nonstationary or nonlinear simulation models. The starting point is the impossibility of using a perfect numerical simulation technique and the need for making use of ever limited computer facilities in order to achieve, in the best possible way, the stochastic realizations desired. The analysis of numerical

random wave simulation problems in the time and frequency domain, contrasting different simulators, permits the establishing of a relationship between these techniques. The estimation of theoretical divergence produced by each one permits the establishing of general criteria for selecting the suitable technique. Many random wave simulation techniques can be used with different requirements but only a few of them are really justified for each determined case.

SIMULATION MODELS

This paper concentrates on the linear (Gaussian) ergodic (stationary) stochastic model for describing the random ocean wave field. The principles of irregular wave simulation using digital computers will be described.

Borgman(2) has noted two different ways of achieving simulated realizations of a desired linear stochastic process. The first is the digital filtering of white noise by a predicted filter, and the second is the wave superposition method.

A simulator by digital filtering of white noise describes ocean waves by an autoregressive-moving average model (ARMA). This ARMA model can be considered the most general way of describing ocean waves employing digital filtering techniques. The time series generated under this principle will satisfy the following general equations:

$$\eta(t) = \eta(n \Delta t) = z_n \quad ; n=1,2,3,\dots \quad \dots\dots\dots (1)$$

$$z_n = \phi_1 z_{n-1} + \phi_2 z_{n-2} + \dots + \phi_p z_{n-p} + w_n - \Theta_1 w_{n-1} - \dots - \Theta_q w_{n-q} \quad \dots\dots\dots (2)$$

where z_n is the time series generated, w_n is a white noise time series with a variance of σ_w^2 , ϕ_k are p autoregressive parameters, and Θ_m are q moving average parameters. The particular model described by Eqs. (1) and (2) in which p and q orders are fixed, is called ARMA(p,q); it can produce stationary realizations of Gaussian stochastic processes if the two sets of parameters ϕ_k and Θ_m satisfy

the stationary conditions (see Box and Jenkins(3)). The stationary Gaussian time series produced by this model can be considered random realizations belonging to the ensemble of the stochastic process. The stationary linear stochastic process for describing the sea state would be defined exactly by its continuous variance spectrum, $S_{\eta\eta}(f)$. From Box and Jenkins(3) and Bendat and Piersol(1) the following can be written:

$$\psi(B) = (1 - \Theta_1 B - \dots - \Theta_q B^q) / (1 - \phi_1 B - \dots - \phi_p B^p) \quad \dots \dots \dots (3)$$

$$S_{\eta\eta}(f) = 2 \frac{\sigma_w^2}{\omega} \Delta t \left| \psi[\exp(-i2\pi f \Delta t)] \right|^2 = 2 \frac{\sigma_w^2}{\omega} \Delta t |H(f)|^2; 0 < f < 1/(2 \Delta t) \quad \dots (4)$$

Annotations for (4):
 - ψ : psi
 - $\exp(-i2\pi f \Delta t)$: $i = \sqrt{-1}$, imaginary unit
 - $\psi[\dots]$: brackets
 - $| \dots |^2$: modulus
 - σ_w^2 : capital sigma
 - $0 < f < 1/(2 \Delta t)$: less than

$$S_{\eta\eta}(f) = 2 \frac{\sigma_w^2}{\omega} \Delta t \frac{\left| 1 - \sum_{m=1}^q \Theta_m \exp(-im \Delta t 2\pi f) \right|^2}{\left| 1 - \sum_{k=1}^p \phi_k \exp(ik \Delta t 2\pi f) \right|^2}; 0 < f < 1/(2 \Delta t) \quad \dots \dots \dots (5)$$

where B is the backward shift operator, $\psi(B)$ is the transfer function of the linear system ARMA(p,q); H(f) is the frequency response function, Δt is the time interval, ϕ_k and Θ_m the autoregressive and moving average parameters, σ_w^2 the variance of the white noise input and $S_{\eta\eta}(f)$ the variance spectrum of the time series generated by this linear system.

Looking at this from the frequency domain, the variance spectrum $S_{\eta\eta}(f)$ of the output signals has been obtained by the product of the white variance spectrum of the input and the squared frequency response function of the linear system, $|H(f)|^2$. At the same time, in the time domain, it can be considered that the output signal, $\eta(t)$, has been achieved by a convolution of the input signal, $w(t)$, and the impulse response function of the linear system, $h(t)$, which is the inverse Fourier transform of the frequency response function, H(f).

Fryer and Wilkie(9) and Dedow, Thompson and Fryer(4) have proposed efficient applications of the filtering techniques based on the use of a pseudo-random

binary sequence as white noise and employing only moving average parameters in order to achieve a simpler design of the filter's impulse response function. Houn and Overvik(21) have noted the advantages of filtering simulation techniques in order to produce a generation of a time series directly from real wave ARMA parameters which are estimated by the criterion of maximum entropy(MEM). And they also noted the possibility of assuming a spectral shape for the process to determine the ARMA parameters that would fit the variance spectrum, defined by Eq.(5), to the spectral shape desired. The digital filtering of white noise seems to be the most common technique for generating waves in model flumes. But Goda(13) has pointed out that a series representation with trigonometric functions has some advantages in comparison with the digital filtering techniques, especially for numerical simulation by computer in which the role of the phase information is important.

A simulator by wave superposition describes ocean waves by component summation. The realizations generated satisfy

$$\eta(t) = \sum_{m=1}^M R_m \cos(2\pi f_m t + \theta_m) \quad \dots\dots\dots (6)$$

↙ capital sigma
↙ theta

$$z_n = \eta(n \Delta t) = \sum_{m=1}^M R_m \cos(2\pi f_m n \Delta t + \theta_m) ; 0 < f_m < 1/(2 \Delta t) \quad \dots\dots\dots (7)$$

where z_n is a random time series of the ensemble corresponding to the simulated stochastic model, M is the number of wave components, R_m are the M amplitudes of the wave components, f_m are the M frequencies, and θ_m are the M random phase angles distributed uniformly in the interval $U(0, 2\pi)$. The one-dimensional wave superposition method described by Eq.(7) can generate stationary realizations of an approximately Gaussian stochastic process if M is a large number and the R_m amplitudes are not too unbalanced. The time interval, Δt , is related to the maximum frequency imposed by the aliasing condition, and the one-sided variance

spectrum for the process described by Eq. (7) can be written

$$S_{\hat{\eta}\hat{\eta}}(f) = \sum_{m=1}^M \left(\frac{R_m^2}{2} \right) \delta(f-f_m) \quad ; 0 < f_m < 1/(2 \Delta t) \quad \dots \dots \dots (8)$$

in which $\delta(f-f_m)$ is Dirac's delta function centered on the point $f=f_m$.

The relationship which is commonly used to convert a variance spectrum to the amplitude spectrum R_m is

$$S_{\hat{\eta}\hat{\eta}}(f_m) \Delta f_m = R_m^2/2 \quad ; 0 < f_m < 1/(2 \Delta t) \quad \dots \dots \dots (9)$$

where Δf_m is the frequency interval related to the frequency component f_m and the variance spectrum, $S_{\hat{\eta}\hat{\eta}}(f)$, defines the stationary Gaussian stochastic process to be simulated. Borgman(2) and Goda(15) showed two of this models by wave superposition based on Eqs. (7) and (9); later, Goda(14) modified the Eq.(9) to explain the variability of statistics of surface sea elevation, taking into consideration the directionality of ocean waves.

A directional simulator by wave superposition describes ocean waves by a component summation such as in a one-dimensional case. The directional time series of random surface must satisfy

$$\eta(x,y,t) = \sum_{m=1}^M \sum_{l=1}^L R_{ml} \cos \left[k_m x \cos(\alpha_0 - \alpha_1) + k_m y \sin(\alpha_0 - \alpha_1) + \theta_{ml} - 2\pi f_m t \right] \quad \dots \dots \dots (10)$$

$$z_n^{\hat{\eta}} = \eta(x_0, y_0, n \Delta t) = \sum_{m=1}^M \sum_{l=1}^L R_{ml} \cos \left[k_m x_0 \cos(\alpha_0 - \alpha_1) + k_m y_0 \sin(\alpha_0 - \alpha_1) + \theta_{ml} - 2\pi f_m n \Delta t \right] \quad ; 0 < f_m < 1/(2 \Delta t) \quad \dots \dots (11)$$

where (x,y) are the coordinates of the point in which the time evolution of the wave surface $\eta(x,y,t)$ is simulated, R_{ml} are the amplitude components of the waves with k_m wave numbers, f_m frequencies and α_1 angle directions; θ_{ml} are random

phases uniformly distributed in $U(0, 2\pi)$ interval, M is the number of frequency components, L is the number of direction components for each frequency and z_n is the one-dimensional time series of sea elevations at the point defined by the (x_0, y_0) coordinates. The wave number k_m is usually presumed to satisfy the relationship

$$(2\pi f_m)^2 = gk_m \tanh(k_m h) \dots\dots\dots (12)$$

in which h denotes the water depth. The relationship between the amplitude of wave components and the directional variance spectrum commonly used is

$$S_{\eta\eta}(f_m, \alpha_1) \Delta f_m \Delta \alpha_1 = R_{m1}^2 / 2 \dots\dots\dots (13)$$

where $S_{\eta\eta}(f, \alpha)$ is the wave directional spectrum, Δf_m are the frequency component intervals, α_1 are the angle intervals of the direction components and R_{m1} the amplitude of the wave components.

Goda(14) also showed that the one-dimensional time series generated by Eq.(11) could be understood as having been generated by Eq.(7) in which R_m would be a random variable with average value and standard deviation as defined by Eq.(14). The squares of R_m divided by $S_{\eta\eta}(f_m) \Delta f_m$ would be a random variable with a chi-squared distribution with two degrees of freedom and with the presumption of a sufficiently large number of directional components, L . This is to say

expected value

$$E[R_m^2] = 2 S_{\eta\eta}(f_m) \Delta f_m ; m=1, 2, \dots, M \dots\dots\dots (14)$$

$$R_m^2 = c_m S_{\eta\eta}(f_m) \Delta f_m ; m=1, 2, \dots, M \dots\dots\dots (15)$$

The random variable c_m has a chi-squared distribution with two degrees of freedom, $\chi^2(2)$. The probability density function of the amplitude components R_m could be calculated by Eq.(17) in the following manner:

$$p(c_m) = \frac{1}{2} \exp(-\frac{1}{2}c_m) ; c_m > 0 \quad \dots\dots\dots (16)$$

$$p(R_m) = \frac{R_m}{S_{\eta\eta}(f_m) \Delta f_m} \exp\left(-\frac{1}{2} \frac{R_m^2}{S_{\eta\eta}(f_m) \Delta f_m}\right) ; R_m > 0 \quad \dots\dots\dots (17)$$

The probability density function of R_m is a Rayleigh function in which the mean and standard deviation can be calculated by

expected value

$$E(R_m) = \left(\frac{1}{2} \pi S_{\eta\eta}(f_m) \Delta f_m\right)^{1/2} \quad \dots\dots\dots (18)$$

standard deviation

$$\sigma(R_m) = \left[(2 - \frac{1}{2} \pi) S_{\eta\eta}(f_m) \Delta f_m\right]^{1/2} \quad \dots\dots\dots (19)$$

where the assumption of a great number of wave components with the same frequency, different directions of propagation and random phases are made to explain the random sea elevations producing a double random model for random sea simulations.

The two main groups of random wave simulators have advantages and disadvantages for solving different problems. Digital filtering techniques have the advantages of easy implementation, high velocity and adaptability to ocean wave analysis made with parametric methods of spectral estimation. On the other hand, flexibility, adaptability to any spectral shape and extensive use of nonparametric techniques of spectral estimation are advantages of wave summation simulation techniques. The random wave generation techniques for laboratory tests have specific problems related to the generation of the required signals and the conditions of the response of the equipment available. Funke and Mansard(10) have recently proposed a classification of these simulators in deterministic and probabilistic groups in which the wave generation techniques used by most laboratories in the world are included.

NUMERICAL SIMULATION TECHNIQUES

The numerical linear simulation techniques of one-dimensional random wave

models are the particular methods for generating, by digital computer, time series associated with the wave energy spectrum $S_{\eta\eta}(f)$ that defines each random sea model. In the same way, a directional random sea model can be described by its directional wave energy (variance) spectrum, $S_{\eta\eta}(f, \alpha)$.

If the ergodic-stationarity and Gaussian-linearity stochastic properties for a random wave model are assumed, the process can be defined exactly by its variance spectrum $S_{\eta\eta}(f)$ for one-dimensional problems or $S_{\eta\eta}(f, \alpha)$ for directional cases. Considering one-dimensional numerical simulation by wave superposition techniques, different numerical simulators can be used for achieving a time series corresponding to a given spectrum.

A numerical random sea simulator by the wave components method will be defined by its particular way of solving the simulation described by Eq.(7). The construction of one of these numerical simulation techniques can be understood in five steps: the definition of the variance spectrum whose numerical simulation is possible; the division of the variance spectrum in spectral bands; the accumulation of the band variance in fixed frequencies for each spectral band; the determination of the random phases; and finally, the application of an algorithm for computing the basic method described in Eq.(7).

First step: The variance spectrum of the process can be simulated only to a maximum frequency limit ($f_{\max} = 1/(2\Delta t)$) because the digital realizations are generated with a constant time interval, Δt . Directly from the establishing of the maximum simulation frequency limit or indirectly fixing the time interval for simulation, the fact is that the variance spectrum actually simulated is reduced to a specific frequency range, $f \in (f_{\min}, f_{\max})$, ^{belonging to} which is not always exactly equal to the variance spectrum of the process that should be simulated.

Second step: If the spectral shape of a process that is possible to simulate is decided on, the second step for construction of a specific wave superposition simulator is to divide the basic spectrum into M spectral bands, (f_m, f_{m+1}) , that

must satisfy

$$\bigcup_{m=1}^M (f'_{m, \min}, f'_{m, \max}) = (f'_{\min}, f'_{\max}) \dots \dots \dots (20)$$

where each $(f'_{m, \min}, f'_{m, \max})$ is the range of a spectral band of the total variance spectrum defined in the frequency range, (f'_{\min}, f'_{\max}) . In the time domain this is equivalent to achieving the wave stochastic realizations, defined by $S_{\eta\eta}(f); f \in (f'_{\min}, f'_{\max})$ in the frequency domain, by the addition of M realizations of M independent stationary linear stochastic processes defined by M different band spectra: $S_{\eta\eta}(f); f \in (f'_{m, \min}, f'_{m, \max})$.

Third step: When the spectral shape desired for the process to be simulated is divided into M band spectra, the total variance of each band spectrum must be concentrated in a fixed frequency for each band. In the frequency domain, each band spectrum is reduced to Dirac's delta function spectrum corresponding, in the time domain, to the change of a stochastic realization of a band spectrum process for a sine wave with random phase and the same variance. This can be considered as the band spectra's partial simulations of the process to be simulated, in which the amplitude and phase of each wave component can be calculated

$$f_m : f_m \in (f'_{m, \min}, f'_{m, \max}); m=1, 2, \dots, M \dots \dots \dots (21)$$

$$R_m : \frac{1}{2} R_m^2 = \int_{f'_{m, \min}}^{f'_{m, \max}} S_{\eta\eta}(f) df ; m=1, 2, \dots, M \dots \dots \dots (22)$$

This plan is equivalent to the one expressed by Eq. (9) and can be called a Deterministic Amplitude Component model in a similar way as the Deterministic Spectral Amplitude model(DSA) noted by Tuah and Hudspeth(36).

If each band spectrum were divided into L band spectra with the same frequency range, but with $S_{\eta\eta}(f)/L$ variance spectrum, and each one were reduced to a sine wave with the same frequency $(f_m \in (f'_{m, \min}, f'_{m, \max}))$ but with random phases in the $U(0, 2\pi)$ interval, the resultant wave component would be a sine wave with the same frequency, f_m ; and this component would result in a random amplitude with

a Rayleigh distribution, as defined by Eq. (17), and a random phase uniformly distributed in a $U(0, 2\pi)$ interval. It would give the same result if the one-dimensional sea variance spectrum were considered from a directional sea variance spectrum and if each wave component were considered the result of a L directional wave summation as Eqs.(10) and (11) expressed. These equations refer to Goda's(14) work, assuming that L is sufficiently large for the application of the Central Limit Theorem to the wave superposition. Eqs. (7) and (17) define a Nondeterministic Amplitude Component model, and the one-sided variance spectrum $S_{\eta\eta}(f)$ of the process produced by this simulator is

$$S_{\eta\eta}(f) = \sum_{m=1}^M \frac{1}{2} R_m^2 \delta(f-f_m) = \sum_{m=1}^M \frac{1}{2} c_m^2 [S_{\eta\eta}(f_m) \Delta f_m] \delta(f-f_m) \dots\dots\dots (23)$$

in which c_m is a random variable with $\chi^2(2)$ distribution and $\delta(f)$ is the Dirac's delta function.
(a)
chi-squared

Fourth step: Hudspeth and Min-Chu-Chen(23) have noted that this can be a critical element of the linear simulation technique. An algorithm must be chosen for generating the pseudo-random sequences which require that no reasonable statistical test detects any significant departure from randomness. Perhaps the multiplicative congruential method given by Lehner(26) and generalized by Greenberger(16), as it is defined by Eq. (24), are the most popular methods of generating pseudo-random numbers to carry out Monte Carlo methods (see Zelen and Severo(38) and Hammersley and Handscomb(17)):

$$u_m' = \lambda_1^{(a)} u_{m-1}' + \lambda_2 \quad (\text{modulo } J) \dots\dots\dots (24)$$

J is a large integer and u_m' , λ_1 and λ_2 are integers between 0 and J-1. The numbers $u_m = u_m'/J$ are used as pseudo-random numbers in the $U(0,1)$ interval. The pseudo-random sequence defined by Eq. (24) has a maximum period of J numbers, but the parameters λ_1 , λ_2 and J can be chosen to achieve a very large period

and very low autocorrelations, in which case the usual statistical tests of randomness and uniformness can be easily accomplished.

Fifth step: The algorithm for computing the numerical wave superposition technique chosen has no direct influence on the results of the numerical simulation model considered, but it can considerably affect them. It must be pointed out that only limited computer facilities can be used in each numerical experiment. For this reason an efficient algorithm can permit the use of a better numerical technique with the same simulation method and computer facilities consumed. Reducing the time-consumed for the numerical equations that define the simulation technique permits an increase in the number of wave components, the number of data points simulated and the number of realizations for each numerical experiment or other desired simulation characteristics.

Therefore the most efficient algorithm in each case must be used in order to save the maximum computer facilities and to achieve the best numerical experiment. The first writer(29), using the simple algorithm showedⁿ in Eqs. (27) and (28) for computing the Eq.(7), found satisfactory results for economizing time-consumed against the direct use of the COS(X) function (32/4 ratio) and Goda's(13) fast algorithm (32/13 ratio). The ratio of time-consumed can change depending on the computer, the software, and characteristics of the numerical experiment (especially for one or two-dimensional simulations). The Eqs. (25) and (26) describe Goda's(13) fast algorithm, especially for computing two-dimensional random waves, while the algorithm described by Eqs. (27) and (28) points out the second-order autoregressive behaviour of a sine function.

$$\begin{aligned} \cos(2\pi f_m(n+1)\Delta t) &= \cos(2\pi f_m n \Delta t) \cos(2\pi f_m \Delta t) - \\ &\quad - \sin(2\pi f_m n \Delta t) \sin(2\pi f_m \Delta t) \quad \dots\dots\dots (25) \end{aligned}$$

$$\begin{aligned} \sin(2\pi f_m(n+1)\Delta t) &= \sin(2\pi f_m n \Delta t) \cos(2\pi f_m \Delta t) + \\ &\quad + \cos(2\pi f_m n \Delta t) \sin(2\pi f_m \Delta t) \quad \dots\dots\dots (26) \end{aligned}$$

$$\cos(2\pi f_m(n+2)\Delta t) = d_m \cos(2\pi f_m(n+1)\Delta t) - \cos(2\pi f_m n \Delta t) \quad \dots\dots\dots (27)$$

$$d_m = 2 \cos(2\pi f_m \Delta t) \quad \dots\dots\dots (28)$$

On the other hand, we can use FFT algorithms to achieve simulations of discrete random time sequences by initializing a complex vector in the frequency domain of a FFT algorithm and inverting the Fourier transform back to the time domain. This can be considered a special technique for computing Eq.(7) in the cases where the following equations are fulfilled:

$$f_m = m \Delta f = m / (N \Delta t) \quad ; m=1, 2, \dots, \frac{1}{2}N-1 \quad \dots \dots \dots (29)$$

$$M = \frac{1}{2}N - 1 \quad \leftarrow \left[\left(\frac{N}{2} \right) - 1 \right] \quad \dots \dots \dots (30)$$

where N is the number of data points simulated and Δf is the frequency interval. The characteristics of the FFT algorithm reduce time-consumed, especially if N is a power of two (e.g. 4096, 8192). The Tuah and Hudspeth(36) technique of filtering in the frequency domain simulations based on a Rice's representation of Gaussian noise currents can also be understood as a special algorithm for computing the basic numerical model for Eq.(7). The complex valued FFT coefficients, A_m, may be computed for DSA simulation (R_m deterministic) by

$$A_{m+1} = \frac{1}{2} R_m \exp(+i \theta_m) = \left[\frac{1}{2} S_{\eta\eta}(f_m) \Delta f \right]^{1/2} \exp(+i \theta_m) \quad ; m=1, 2, \dots, \frac{1}{2}N-1 \quad \dots \dots (31)$$

as in Eq.(7). For Nondeterministic Spectral Amplitude simulations(NSA), the amplitudes R_m are random variables with Rayleigh distribution and the set of FFT coefficients, A_m, can be computed

$$A_{m+1} = \frac{1}{2} R_m \exp(+i \theta_m) = \left[c_m S_{\eta\eta}(f_m) \Delta f / 4 \right]^{1/2} \exp(+i \theta_m) \quad ; m=1, 2, \dots, \frac{1}{2}N-1 \quad (32)$$

where c_m is a random variable with χ²(2) distribution. These complex valued NSA-FFT coefficients, A_m, can also be obtained, benefiting the relationship between the χ²(2) and the uniformly distributed random numbers.

$$A_{m+1} = \left[-\frac{1}{2} \ln(u_m) S_{\eta\eta}(f_m) \Delta f \right]^{1/2} \exp(+i \theta_m) \quad ; m=1, 2, \dots, \frac{1}{2}N-1 \quad \dots \dots \dots (33)$$

in which u_m are random uniformly distributed numbers in the interval U(0,1).

Depending on the computer and software available, the algorithm described by Eq.(33) can be more efficient than the one described in Eq.(32).

DISTORTION OF THE RANDOM PROCESS

At first we wanted to simulate a stationary Gaussian(linear) stochastic process defined by its continuous variance spectrum, $S_{\eta\eta}(f)$, in the range $f > 0$. From this theoretical process to the one which can be generated by a numerical simulation technique there are some differences that depend on the numerical method used. This loss of information about the original process imputable to the numerical simulation technique used will be analyzed in this study.

First of all, we will point out the large number of theoretical sea spectra used for numerical simulation experiments defined in the entire frequency range, $f > 0$, with an asymptote potential tail, $\beta_5 f^{-5}$ (see Pierson and Moskowitz(32) and Hasselman et al.(18) for PMK and JONSWAP spectra). This is true because of Kitaigorodskii's similarity law and the dimensional analysis based on Phillips'(31) ideas of an equilibrium range in the wave spectrum.

A problem associated with this type of sea spectra defined for the entire frequency range, $f > 0$, is the infinite spectral moment for orders up to and including 4. This fact produces a theoretical inconsistency by which the spectral bandwidth parameter, ϵ , would always be $\epsilon=1$, and the mean wave period, \bar{T} , would be zero for Bretschneider, Pierson, Moskowitz, ITTC and ISSC spectra, as Denis(5) has noted. Denis(5) proposes resolving this inconsistency by determining the cut-off-frequency where gravity waves first make their appearance, and the frequency where the variance spectrum is determined by viscous action, and then studying spectral shapes related to different mechanisms of wave generation-propagation. It must be remembered that Phillips(31) pointed out the restrictions for wave numbers and frequencies in order to apply the idea of an equilibrium range in the sea spectrum, and Kitaigorodskii's law is based on restrictive conditions

in which the water surface stress and viscosity are not considered.

Another way of spotting possible incongruences in the model is by studying the relationship between spectral moments and derived time series. The variance spectra of the derivative processes are related to $S_{\hat{\eta}\hat{\eta}}(f)$, if $\eta(t)$ is the surface elevation, $\dot{\eta}(t)$ is the vertical velocity of sea surface, $\ddot{\eta}(t)$ is the vertical acceleration and $\eta^{(k)}(t)$ is the kth derivative of $\eta(t)$, in the following way:

$$S_{\hat{\eta}'\hat{\eta}'}(f) = (2\pi)^2 f^2 S_{\hat{\eta}\hat{\eta}}(f) ; \dot{\eta}(t) = d\eta(t) / dt \quad \dots\dots\dots (34)$$

double eta prime S

$$S_{\hat{\eta}''\hat{\eta}''}(f) = (2\pi)^4 f^4 S_{\hat{\eta}\hat{\eta}}(f) ; \ddot{\eta}(t) = d^2\eta(t) / dt^2 \quad \dots\dots\dots (35)$$

double eta double prime

$$S_{\hat{\eta}^{(k)}\hat{\eta}^{(k)}}(f) = (2\pi)^{2k} f^{2k} S_{\hat{\eta}\hat{\eta}}(f) ; \eta^{(k)}(t) = d^k\eta(t) / dt^k \quad \dots\dots\dots (36)$$

double eta super k

where $S_{\hat{\eta}'\hat{\eta}'}(f)$, $S_{\hat{\eta}''\hat{\eta}''}(f)$, and $S_{\hat{\eta}^{(k)}\hat{\eta}^{(k)}}(f)$ are the variance spectra of the vertical velocity, vertical acceleration and k-derivative function of vertical displacement of sea surface at a given point. If the fourth spectral moment is infinite, it means that the zeroeth spectral moment of the vertical acceleration process is infinite, and therefore the variance of vertical acceleration is also infinite. The kinematic and dynamic stability conditions for sea waves are inconsistent with high vertical accelerations for the sea surface. The variance spectrum of vertical displacement must be cut or modified for high frequencies in order to achieve finite spectral moments for all orders. This is not only a condition imposed by digital computer numerical methods, but it is also a necessary method for achieving a minimum consistency with the linearity property assumed for the stochastic model.

On the other hand, it can be affirmed that the direct measures ^{of} on real sea waves are usually analyzed below a cut-off-frequency of about 0.7 Hz . The Pierson and Moskowitz spectrum(32) was derived from spectra estimated over the frequency range 0 to 0.33 Hz ; the JONSWAP spectrum(18) was derived from a variety

of wave instruments with high-frequency cut-offs between 0.7 to 1 Hz ; Forristall(8) has studied the measurements of saturated range in ocean wave spectrum with recorder and processing systems that had frequencies of less than about 0.7 Hz ; and Scott's spectrum(34) was derived from Pierson-Moskowitz's spectral estimations fitting Darbyshire's formulation truncated at a frequency of 0.33 Hz. For the frequency range between 0 and about 0.2 Hz, the recording systems commonly used can give a reasonable support ^{of} to an empirical formulation of $S_{\eta\eta}(f)$, and the spectral shape in the frequency range of about 0.2 to 0.7 Hz interval can be specifically studied in order to achieve reasonably well fitted tails such as $\beta_5 f^{-5}$. But the viscous action in the fluid motion appears in frequencies over 0.7 Hz . As of this frequency one can suppose that a f^{-5} law (Forristall(8)) is positive; or there is a special shape within the range in which the viscous action is present (Denis(5)); or there is a non-equilibrium state as Garret(11) proposed, using sensors with cut-off frequencies of about 3 Hz . The nonlinear effects, the characteristics of the frequency response functions of the available wave recorders and the questionable importance of the spectral shape in the frequency range over 0.7 Hz can support an arbitrary cut-off-frequency for the numerical random sea simulators.

The theoretical sea spectrum desired will be modified for numerical simulation because the cut-off-frequency will be directly determined by some criterion or, indirectly, by the time interval chosen, Δt . The information of the frequency range lost will produce distortions on some parameters which will change their original values. Table 1 shows the evolution of the σ_{η}^2 , $\sigma_{\eta'}^2$, $\sigma_{\eta''}^2$, and \bar{T}_0 associated with a PMK sea spectrum ($m_0 = 66.5$ sq ft (6.19 m²), $f_p = 0.0635$ Hz) for different cut-off frequencies. It can be observed that an arbitrary cut-off-frequency cut over 0.5 Hz does not affect the elevation variance, σ_{η}^2 , the velocity variance, $\sigma_{\eta'}^2$, and the mean wave period, $\bar{T}_0 = (m_0/m_2)^{1/2}$ as these are not related to the fourth spectral moment. However the spectral bandwidth parameter, ϵ , and the acceleration

variance, $\hat{\sigma}_{\eta}^2$, are ^{quite} very distorted by the chosen cut-off-frequency. Rye(33) has also shown the instability of some currently used wave parameters with respect to the cut-off-frequency. An arbitrary cut-off-frequency can be justified in some cases, but it must be taken into consideration in order to determine which parameters can be employed and their associated initial level of distortions.

Secondly, the sea spectrum that can be simulated, $S_{\eta\eta}(f); f \in (f_{\min}, f_{\max})$, could be considered added M band spectra due to the linearity property of the theoretical model. This step does not introduce any distortion in the numerical model.

Thirdly, if each stochastic component of each spectral band is simulated by a single sine wave with random phase and amplitude related to the variance of the band spectrum, the stochastic component irreversibly loses the information about the process contained in its original continuous spectral shape. The simulation of a process with continuous spectrum would need a time series for an infinite duration, which is impossible to achieve. In the frequency domain each band spectrum (Fig. 1-a) is replaced by a Dirac delta function spectrum (Fig. 1-b) defined by a fixed frequency, f_m , and included in the frequency range of the band, (f_m', f_{m+1}') , where each has a variance related to the variance of the band spectrum as a result of the deterministic or probabilistic relationships pointed out in Eqs. (9) and (15). In the time domain, each stochastic component defined by a band spectrum (Fig. 1-c) would be changed by a sine wave function (Fig. 1-d).

The information about the original process lost in this step depends on the method used to divide the sea spectrum and the method used to determine the representative frequency of each band. Borgman(2) and Goda(13,14) have used a regular spectral discretization in order to obtain the same variance for all spectral bands, while Goda(15) used a random method for spectral division in order to obtain additional flexibility in the numerical model. Many other kinds of discretization methods can be employed, such as spectral division in constant frequency intervals when used for the application of FFT algorithms. The representative frequency of each band, f_m , must be a type of frequency average of

the frequency range interval's limits, $(f_{m,m+1}^V, f_{m,m+1}^V)$, such as in the case of the arithmetic mean frequency

$$f_{\hat{m}} : f_{\hat{m}} = \frac{1}{2} (f_{m,m+1}^V, f_{m,m+1}^V) ; m=1, 2, \dots, M \quad \dots \dots \dots (37)$$

(for)
or the median variance frequency

$$f_{\hat{m}} : \int_{f_{\hat{m}}^V}^{f_{\hat{m}}} S_{\eta\eta}(f) df = \int_{f_{\hat{m}}}^{f_{m+1}^V} S_{\eta\eta}(f) df ; m=1, 2, \dots, M \quad \dots \dots \dots (38)$$

None of these frequency averages can be considered a correct method for determining the representative frequency of each band spectrum. The arithmetic mean frequency used by Borgman(2) and Goda(15) does not consider the distribution of variance in the frequency range of each band, and the median variance frequency used by Goda(13,14) does not consider the dispersion of the variance in the band spectrum. All methods of frequency average of spectral discretization have serious theoretical inconsistencies to carry out stochastic process simulations, theoretically defined by a specific continuous one-sided variance spectrum, $S_{\eta\eta}(f); f \in (f_{\min}, f_{\max})$.

Fourthly, the generator for pseudo-random numbers can not produce strict random sequences because they are deterministic sequences related to a specific type of generation. It would be necessary to produce infinite random numbers and to perform infinite statistical tests on these numbers in order to guarantee the property of randomness. Hull and Dobell(24) ^(have) ⁿ showed some arbitrary acceptance criteria which are based on several statistical tests. And they noted that a succesful passing of these tests may be considered a necessary, but not ^(a) sufficient condition. If the sequences generated pass several reasonable tests which are designed to reflect the requirements of the simulation problem, such as uniform distribution and independence properties, and if evidence about the poor local behaviour of the pseudo-random sequences has not been located, and if all reasonable precautions about the subroutines used have been taken, one may reasonably assume that this step produces no significant distortion.

Fifthly, it has been noted that the numerical algorithms for computing a specified numerical simulation technique do not directly produce distortions of the simulation method, but rather distortions are indirectly produced. The most efficient algorithm used by the first writer(29) to compute Eq. (7) was that defined by Eqs.(27) and (28). For numerical simulations via FFT algorithms, a double unstacked algorithm was used because only the time-consumed was considered. The wave superposition method given by Eqs. (7),(29) and (30) can be expressed in the frequency domain by

capital letter

$$Z_m^{\wedge} = \frac{1}{2} R_m^{\wedge} \exp(+i \theta_m^{\wedge}) \quad ; m=1, 2, \dots, \frac{1}{2}N-1 \quad \dots \dots \dots (39)$$

asterisk

$$Z_{N-m}^{\wedge} = Z_m^{\wedge*} \quad ; m=1, 2, \dots, \frac{1}{2}N-1 \quad \dots \dots \dots (40)$$

where Z_m^{\wedge} are the discrete Fourier transform of the time series, z_n^{\wedge} . Two processes can be simulated at the same time by locating the time series in the real and imaginary parts of a complex time series :

$$z_n^{\wedge} = z_{1n}^{\wedge} + i z_{2n}^{\wedge} \quad ; n=1, 2, \dots, N \quad \dots \dots \dots (41)$$

z_n^{\wedge} is the complex array in the time domain. If $R_{1m}^{\wedge}, R_{2m}^{\wedge}$ and $\theta_{1m}^{\wedge}, \theta_{2m}^{\wedge}$ are the amplitudes and phases corresponding respectively to the processes z_{1n}^{\wedge} and z_{2n}^{\wedge} , the Fourier transform of this complex time series can be expressed by

$$Z_m^{\wedge} = \frac{1}{2} (R_{1m}^{\wedge} \cos \theta_{1m}^{\wedge} - R_{2m}^{\wedge} \sin \theta_{2m}^{\wedge}) + i (R_{2m}^{\wedge} \cos \theta_{2m}^{\wedge} + R_{1m}^{\wedge} \sin \theta_{1m}^{\wedge}) \quad \dots \dots \dots (42)$$

$$Z_{N-m}^{\wedge} = \frac{1}{2} (R_{1m}^{\wedge} \cos \theta_{1m}^{\wedge} + R_{2m}^{\wedge} \sin \theta_{2m}^{\wedge}) + i (R_{2m}^{\wedge} \cos \theta_{2m}^{\wedge} - R_{1m}^{\wedge} \sin \theta_{1m}^{\wedge}) \quad \dots \dots \dots (43)$$

$$Z_0^{\wedge} = Z_{\frac{1}{2}N}^{\wedge} = 0 \quad ; z_n^{\wedge} = \text{DFT}^{-1}(Z_m^{\wedge}) \quad ; m=1, 2, \dots, \frac{1}{2}N-1 \quad \dots \dots \dots (44)$$

Using the Eqs. (7),(29),(30) and either (9) or (15), this complex array

for deterministic or nondeterministic amplitude methods can be directly constructed in the frequency domain, and afterwards a FFT algorithm can directly give us the complex array in the time domain with realizations of two stochastic and independent time series which correspond to real and imaginary parts. Hudspeth and Borgman(22) have presented an explanation for the construction of unstacked FFT and stacked algorithms which are especially appropriate for minicomputers. The relative efficiency between the FFT and the algorithm described by Eqs. (27) and (28) depends on the hardware and the software available in each case; the first writer(29) consumed approximately equal time on a number of wave components $M=32(\log N)/(\log 2048)$, in which N is the number of points to be simulated.

CRITERIA FOR QUALIFYING

The distortions associated with each numerical random sea simulation technique, and which has proved to be impossible to eliminate for numerical experiments, induces one to plan these techniques from another point of view. If it is necessary to use a numerical simulation technique, and each is incorrect in a strict sense, general criteria for qualifying all numerical simulators must be established in order to get the best one for each problem. With some fixed computer facilities and a given problem the best numerical method can be selected by using the general criteria and admitting the simultaneous distortions related to it.

A numerical one-dimensional linear random sea simulation technique by wave superposition can only produce realizations corresponding to stationary Gaussian stochastic processes defined by Eqs. (8) or (23), which are somewhat similar to the continuous sea spectrum proposed for simulation, $S_{\eta\eta}(f)$. The ideal case would be the unrestricted use of an infinite number of wave components, $M \rightarrow \infty$, as was earlier mentioned.

The analysis of simulators in the frequency domain can point out characteristics difficult to observe in the time domain. Goda(15) specified two appro-

appropriate properties for numerical random sea simulators. That is to say, the set of frequencies, f_m , should not constitute harmonics between each other, and it would be desirable that the amplitude of each component wave ^{be} is approximately equal in magnitude. For common spectral shapes, Borgman's(2) technique for discretization produce wave components with the same amplitude, but they do not constitute harmonics between each other (Fig. 2-b). The FFT simulators can only produce periodic random time sequences because the wave components are harmonics (Fig. 2-c).

It is reasonable to assert that a numerical sea simulation technique must generate nonperiodic realizations because the theoretical variance spectrum, $S_{\eta\eta}(f)$, is a continuous function in the general case. For that reason, an adequate property would be when the frequency component does not constitute harmonics so that synthetic registers have an infinite or almost-infinite period. The simulators with FFT algorithm like the one showed ⁿ in Eqs. (42), (43) and (44) can only produce N-periodic random time series. These simulators would be rejected by this criterion in opposition to classic simulators such as Borgman's and Goda's method using non-harmonic component waves.

It is reasonable to affirm that a numerical sea simulation technique must generate nondeterministic realizations because the theoretical process is considered a Gaussian ergodic stochastic process, and a none simulated point can be exactly predicted from the knowledge of the rest of its time series. With this criterion a realization simulated via FFT can be entirely predicted knowing N points. And this will reproduce a recurrent N, N being the length of the complex array in an unstacked algorithm or a double length for one which is stacked. However, the classical non-harmonic wave summation techniques are not preferable under this criterion because a digital sine wave can be considered a deterministic, second-order, special autoregressive realization as shown in Eqs. (27) and (28). This can be written in the following manner:

$$\hat{z}_{m(n+2)} = d_m \hat{z}_{m(n+1)} - \hat{z}_{m(n)} ; m=1,2,\dots,M \text{ and } n=1,2,\dots \quad (45)$$

where d_m is determined by Eq.(28), depending on the time interval, Δt , and the wave frequency, f_m , and $\hat{z}_{m(n)}$ correspond to the wave frequency, f_m , and the time, $N \Delta t$. A summation function of M sine waves can be considered a special 2M-order autoregressive deterministic realization because each discrete sine wave can be exactly predicted from two starting points and the frequency factor, d_m . So a wave superposition simulation method has only 2M nondeterministic points, where M is the number of wave components. This criterion permits one to conclude that the best method is that which has the largest number of wave components. Therefore the methods based on FFT algorithms would be preferred, especially if N is a power of two (see Witting and Sinha(37) related to Shinozuka(35)).

It is also reasonable to assert that a numerical sea simulation technique must generate realizations corresponding to a stochastic process with spectral moments almost-equal to the one theoretically designed. The properties of the variance spectrum and the time series related to it can be defined by the spectral moments of the process, and it is also necessary to support a minimum coherence among derivative processes that can be simulated in the same numerical experiment. If this noted criterion is taken into account, a good simulator could be made resolving

$$\sum_{m=1}^M \left(\frac{1}{2} R_m^2 \right) f_m^{2k} = m_k ; k=k_0+1, k_0+2, \dots, k_0+2M \quad (46)$$

etc.

where R_m are the M wave amplitudes, f_m are the wave frequencies and the m_k are 2M spectral moments chosen to be equalized between the theoretical spectrum and the process actually simulated. If the M wave frequencies are previously fixed, the 2M nonlinear equations given by Eq.(46) can be reduced to M linear equations, and M spectral moments could be equalized. If a spectral discretization is fixed and the frequency bands are determined as in Eqs.(20),(21) and (22), only an equal zeroeth spectral moment between the theoretical and simulated process can

took

be guaranteed. Nagai(30) has taken the frequency representing each band spectrum in such a way that the second spectral moment was also guaranteed.

Three deterministic amplitude wave superposition simulators and one non-deterministic amplitude wave superposition were contrasted, and subsequently denominated B1, B2, DSA and NSA respectively. The B1 and B2 are deterministic amplitude non-harmonic frequency wave superposition simulation techniques that utilize Borgman's method of spectral discretization given in Eq. (22), and in which all the amplitudes R_m are equal. The B1 simulator has a band frequency given in Eq.(38) (median variance frequency), and B2 has a band frequency given by Eq. (37) (arithmetic mean frequency). The simulators denominated DSA and NSA are two FFT simulators with deterministic and nondeterministic amplitude components shown in the frequency domain by Eqs.(31) and (33) respectively.

It must be noted that a nondeterministic amplitude simulator generates a stochastic process with all spectral moments, m_k , scattered about the ones obtained by the deterministic amplitude simulator; the arithmetic means are equal for each moment and their standard deviations can be calculated

$$\sigma(m_k) = \left(\frac{1}{2} \nu_k \right)^{1/2} E(m_k) = \left(\frac{1}{2} \nu_k \right)^{1/2} \frac{\left(\sum_{m=1}^M R_m^4 f_m^{2k} \right)^{1/2}}{\sum_{m=1}^M R_m^2 f_m^k} \quad E(m_k) = \frac{1}{2} \left(\sum_{m=1}^M R_m^4 f_m^{2k} \right)^{1/2} \quad \dots \dots \dots (47)$$

in which R_m are the deterministic amplitudes of the wave components, f_m are the wave frequencies and ν_k the number of degrees of freedom that can be considered for the χ^2 distribution of each spectral moment variable, m_k .

The choice of spectral discretization and fixed frequency systems based on the equalizing of certain spectral moments may be justified, but it also causes additional time-consumed. It can also be justified if we consider that the available sea wave recorders and digital processing methods produce high uncertainties about the true spectral moments, and therefore it would make no sense to try to equalize many spectral moments.

CONTRAST OF SIMULATIONS

The distortions produced by each numerical random sea simulator induce an obvious result: the stationary Gaussian time series generated by any linear random sea simulator can not have the exact properties desired. The writers (6) have studied some wave parameters associated with time series generated from different simulators (B1,B2; and DSA), and have pointed out significant differences which depend on the number of each simulator's wave components. In table 2 relative mean and standard deviation estimations of some simulated wave parameters are compiled. The root-mean-square of surface elevations, \hat{z}_{rms} , significant wave height, H_s , median wave height, $H_{0.5}$, mean wave period, \bar{T} , and maximum wave height, H_{max} , have been studied. B1,B2,DSA and NSA simulators have been employed with various wave components which are indicated by an integer following the nomenclature (i.e. B1-256 : B1 technique with 256 wave components). The same theoretical variance spectrum and forty realizations have been generated for each case.

To analyze these results one may consider, assuming Gaussianity, that the means estimated oscillate around the exact means with an expected standard deviation of about 16% of the standard deviation estimated from the forty realizations. And the standard deviations estimated oscillate around the exact ones with an expected standard deviation of about 8% of the sample standard deviation estimated. The B1 and B2 simulators have the same random phase sequences for the same number of wave components, so the differences between pairs of these simulations correspond to the different frequency choices in the numerical simulator given in Eqs. (37) and (38). The zero-up-crossing criterion has been used to define the wave characteristics of the sea surface elevations.

Analyzing table 2, a first significant difference can be noted between the nondeterministic amplitude simulations (NSA) and deterministic amplitude simulations (DSA). This is because the double variability of the NSA simulator has influence on the standard deviation of the parameters calculated. A second difference can be indicated with respect to the increase of the dispersion of the \hat{z}_{rms} of surface elevations simulated by deterministic amplitude simulators when the number of wave

components increases. Thirdly, it can be noted from the wave period parameter obtained from realizations generated by B1 and B2 simulators that time series produced by the simulator denominated B1 achieve wave periods which are significantly larger than the ones generated by simulator B2. Other significant differences may be observed because these are realizations which correspond to different stochastic processes as shown in Fig. 3. The simulation parameters are the same for all simulators: variance spectrum $PMK(f_p = 0.0635 \text{ Hz})$, $f_{\min} = 0$, $f_{\max} = 0.5 \text{ Hz}$, and $\Delta t = 0.5 \text{ sec}$.

The spectral leakage in the frequency domain must be noted before analyzing the behaviour of the sea variability. Each wave component considered is only extended by a finite duration, $N \Delta t$, which does not contain an exact number of waves. This will be analyzed in the frequency domain as if it were a superposition of harmonic wave components with phases and amplitudes related to phase, wave frequency and spectral window corresponding to the chosen rectangular time window. From the frequency point of view, the rms of sea elevations calculated from deterministic amplitude simulators show some variability corresponding to the multicomposition of harmonic waves with amplitudes and phases which are, to some respect, random and deterministic. For instance, a DSA-FFT simulator can generate only periodic sequences with exact rms, but it is possible to obtain variability by choosing limited simulations from other larger periodic realizations generated with a DSA simulator. Realizations of 1024 points were extracted from time series of 8192 points generated by a DSA simulator, and the relative mean and standard deviation for rms were estimated in 0.985 and 0.064 respectively (forty realizations). This phenomenon of variability produced by the limited duration of the time series is clearly observed by the increase of the variability produced by simulators with a larger number of wave components.

By contrasting with actual sea record, a reasonable measure of distortions would be obtained for each numerical simulator. However, sea surface movement is a nonstationary process and the actual available records are usually extended for less than twenty minutes. Goda(14) pointed out the great wave variability of

The sea field and dissuaded the use of deterministic amplitude simulators such as B1 or B2. With nondeterministic amplitude component simulators based on the B1-200 model Goda(12) compared the variability of simulated wave parameters to the ones obtained from actual swell data, and he observed that the values of coefficient of variation for wave heights of the observed swell were larger than the numerical model. The variability(standard deviation) of rms sea elevations, z_{rms} , and significant wave height, H_s , were 6.8% and 7.6% respectively, which contrasted Goda's numerical predictions of 5.1% and 5.5% for simulated records of 120 waves. The realizations generated by NSA-FFT simulator produced a variability of rms elevation and significant wave height of about 5% contrasting Goda's 6.8% and 7.6%. But one should consider that the peakedness of real wave spectra measured by Goda(12) was higher than PMK spectrum, and consequently the number of degrees of freedom considered for simulation was excessive. The Eq. (47) can clearly give an idea of the variability expected from a NSA simulation and the influence of the spectral shape on the wave variability.

Donelan and Pierson(7) have studied the variability of spectra of wind-generated waves of two sets of wave data: one from a controlled laboratory experiment and the other from a fixed tower in Lake Ontario. They concluded that the theory of stationary Gaussian processes provides accurate estimates of the sampling variability. Therefore the simulations via NSA-FFT simulator can be accepted in order to describe the random sea variability. But the sea spectrum to be simulated must agree with the actual process, especially for the number of degrees of freedom to be considered. The number of degrees of freedom for a realization generated by a NSA simulator can be calculated

$$\nu_0 = \frac{2 m_0^2}{\int_{f_{min}}^{f_{max}} S_{\eta\eta}^2(f) df} N \Delta t ; 0 \leq f_{min} < f_{max} \leq 1/(2 \Delta t) \dots \dots \dots (48)$$

where ν_0 is the number of degrees of freedom to be considered in order to calculate the variability of the variance of the process, N is the number of points in the sequence analyzed or simulated, Δt the time interval, $S_{\eta\eta}(f)$ the sea spectrum

estimated or to be simulated, and m_0 the variance of the process. The standard deviation for the z_{rms} can be estimated by

$$\sigma(z_{rms}) = \frac{1}{(2 \nu_0)^{1/2}} E(z_{rms}) \dots \dots \dots (49)$$

With respect to the first term in Eq. (49), it may be noted that the parameter expressed in Eq. (50) has time dimension and, to some degree, is a measure for the peakedness of the sea spectrum and the variability of its stochastic realizations

$$\frac{N \Delta t}{\nu_0} = \frac{\int_{f_{min}}^{f_{max}} S_{\eta\eta}^2(f) df}{2 m_0^2} ; 0 \leq f_{min} < f_{max} \leq 1/(2 \Delta t) \dots \dots \dots (50)$$

This parameter remains approximately constant whenever the time interval Δt is sufficiently small.

SUMMARY AND CONCLUSIONS

The numerical simulation techniques for Gaussian ergodic stochastic models applied to the description of random ocean wave field have been analyzed. The continuous one-sided variance spectrum of the sea surface elevations and the series representation with trigonometric functions have been chosen as the two basic elements for description and simulation of random sea processes. The relationships among directional, one-dimensional, deterministic and nondeterministic amplitude component simulation techniques have been studied from the perspective of a practical numerical simulation.

From a general method for the creation of all numerical linear one-dimensional simulators, each numerical wave summation technique has been described. The analysis has been made in the time and frequency domain, dividing the numerical simulator construction into five steps: the establishment of a variance spectrum which is possible to simulate; the division into band spectra; the choice of a representative frequency of band; the generation of pseudo-random sequences; and the choice of algorithms for computing the numerical wave superposition technique chosen. This approach to understanding the wave superposition techniques ^{of} simulation permits one to compare the different numerical techniques from a unique general method.

The undesirable distortions associated with the wave composition simulators are analyzed noting the lack of information about the theoretical process referred to from each step in this simulator construction method. A discussion of the choice of a cut-off-frequency for a theoretical sea elevation spectrum and the relationships among spectral moments from derivative stochastic processes permits one to show the inconsistency of some spectral asymptotic tails for each range of frequency commonly used. All methods of frequency average show serious theoretical inconsistencies in order to carry out correct simulations of a process defined by a continuous spectral function. It is impossible to generate random sequences with a digital computer, so the statistical tests for uniform distribution and independence permit one to guarantee, to some degree, the randomness of the sequences used for simulation. Some efficient algorithms shown can indirectly reduce the level of distortions associated with each numerical simulation technique such as the FFT algorithms.

Three criteria for qualifying one-dimensional wave superposition simulators are justified in order to choose the most appropriate for each numerical experiment. In order to obtain nonperiodic realizations, it is necessary to choose nonharmonic frequencies. And in order to obtain nondeterministic time series of N points, $N/2$ wave components are necessary. The spectral moments of the process simulated must be as approximate to the theoretical ones as possible. And finally, the time-consumed is the last condition to be considered.

The contrast of some numerical simulation techniques commonly used in Monte Carlo experiments have been analyzed in the frequency domain to support the vision of observed distortions and the arbitrariness of some numerical experiments which simulation techniques previously designed have used. For a correct representation of the variability of ocean waves, nondeterministic amplitude component simulators must be used, and the peakedness of the sea spectrum must be considered in order to define the number of degrees of freedom of the estimated or theoretical sea spectrum.

ACKNOWLEDGMENT

The writers would like to thank Yoshimi Goda and Edward Funke for their quite very valuable comments.

APPENDIX I.-REFERENCES

1. Bendat, J.S., and Piersol, A.G., Random Data: Analysis and Measurement Procedures , 1st ed., John Wiley and Sons, Inc., New York, N.Y.,1971.
2. Borgman, L.E., "Ocean Wave Simulation for Engineering Design," Journal of the Waterways and Harbors Division, ASCE, Vol. 95, No. WW4, Proc. Paper 6925, Nov., 1969, pp. 557-583.
3. Box, E.P., and Jenkins, G.M., Time Series Analysis: Forecasting and Control , 2nd ed., Holden-Day, Inc., San Francisco, California,1976.
4. Dedow, H.R.A., Thompson, D.M., and Fryer, D.K., "On the Generation, Measurement and Analysis of Random Seas," presented at the November, 1976, Central Water and Power Research Station Diamond Jubilee Symposium, held at Poona, India.
5. Denis, M.S., "Some Comments on Certain Idealized Variance Spectra of the Seaway Currently in Fashion," presented at the July 2-5, 1980, International Seminar on Criteria for Design and Construction of Breakwaters and Coastal Structures, held at Santander, Spain.
6. Diez, J.J., and Medina, J.R., "Problemas Asociados a la Utilización de los Simuladores Numéricos de Oleaje," Revista de Obras Públicas, Spain, Feb.-Mar., 1983, pp. 89-109.
7. Donelan, M., and Pierson, W.J., "The Sampling Variability of Estimates of Spectra of Wind-Generated Gravity Waves," Journal of the Geophysical Research, Vol. 88, No. C7, May 20, 1983, pp. 4381-4392.
8. Forristall, G.Z., "Measurements of a Saturated Range in Ocean Wave Spectra," Journal of Geophysical Research, Vol.86, No. C9, Sep. 20, 1981, pp. 8075-8084.
9. Fryer, D.K., and Wilkie, M.J., "The Simulation in the Laboratory of Random Seas and their Effects," presented at the September 23-25, Conference

Proceedings on Instrumentation in Oceanography, held at Bangor, U.K. .

10. Funke, E.R., and Mansard, E.P.D., "The NRCC Random Wave Generation Package," Technical Report TR-HY-002, National Research Center of Canada, Division of Hydraulics Laboratory, Ottawa, Canada, Sep., 1983.
11. Garret, J., "Some New Observations on the Equilibrium Region of the Wind-wave Spectrum," Journal of Marine Research, Vol. 27, No. 3, 1969, pp. 273-277.
12. Goda, Y., "Analysis of Wave Grouping and Spectra of Long-travelled Swell," Report of the Port and Harbour Research Institute, Yokosuka, Japan, Vol. 22, No. 1, Mar., 1983. pp.3-41.
13. Goda, Y., "Wave Simulation for the Examination of Directional Resolution," presented at the September, 1981, ASCE & ECORE International Symposium Directional Wave Spectra Applications '81, held at Berkeley, California.
14. Goda, Y., "Numerical Experiments on Statistical Variability of Ocean Waves," Report of the Port and Harbour Research Institute, Yokosuka, Japan, Vol. 16, NO. 2, June, 1977, pp. 3-26.
15. Goda, Y., "Numerical Experiments on Wave Statistics with Spectral Simulation," Report of the Port and Harbour Research Institute, Yokosuka, Japan, Vol. 9, No. 3, Sep., 1970, pp. 3-57.
16. Greenberger, M., "Notes on a New Pseudo-Random Number Generator," Journal of the Association of Computer Machines, Vol. 8, 1961, pp. 163-167.
17. Hammersley, J.M., and Handscomb, D.C., Monte Carlo Methods , 3rd ed., Chapman and Hall, Ltd, London, Great Britain, 1979.
18. Hasselman, K., et al., "Measurements of Wind-wave Growth and Swell Decay During the Joint North Sea Wave Project (JONSWAP)," UDC 551.466.31. ANE German Bright, Deutsches Hydrographisches Institut, Hamburg, Germany, 1973.
19. Hasselman, K., "Nonlinear Interactions Treated by the Methods of Theoretical Physics (with Application to the Generation of Waves by Wind)," Proceedings of the Royal Society, London, Series A, Vol. 299, 1967, pp. 77-100.

20. Hasselman, K., "On the Non-linear Energy Transfer in a Gravity-Wave Spectrum, Part I," *Journal of Fluid Mechanics*, Vol. 12, 1962, pp. 481-500.
21. Houmb, O.G., and Overvik, T., "Some Applications of Maximum Entropy Spectral Estimation to Ocean Waves and Linear Systems Response in Waves," *Applied Ocean Research*, Vol. 3, No. 4, 1981, pp. 154-162.
22. Hudspeth, R.T., and Borgman, I.E., "Efficient FFT Simulation of Digital Time Sequences," *Journal of the Engineering Mechanics Division, ASCE*, Vol. 105, No. EM2, Proc. Paper 14517, April, 1979, pp. 223-235.
23. Hudspeth, ^(R.T.) and Chen, M.C., "Digital Simulation of Nonlinear Random Waves," *Journal of the Waterway, Port, Coastal and Ocean Division, ASCE*, Vol. 105, No. WW1, Proc. Paper 14376, Feb., 1979, pp. 67-85.
24. Hull, T.E., and Dobell, A.R., "Random Number Generators," *Society of Industrial Applied Mathematics Review*, Vol. 4, No. 3, July, 1962, pp. 230-254.
25. Kinsman, B., *Wind Waves*, Prentice-Hall, Inc., Englewood Cliffs, N.J., 1965.
26. Lehmer, D.H., "Mathematical Methods in Large-Scale Computing Units," *Annals of the Computation Laboratory of Harvard University*, Vol. 26, 1951, pp. 141-146.
27. Longuet-Higgins, M.S., "Modified Gaussian Distributions for Slightly Nonlinear Variables," *Radio Science Journal of Research NBS/USNC-URSI*, Vol. 68D, No. 9, Sep., 1964, pp. 1049-1062.
28. Longuet-Higgins, M.S., "The Effect of Non-linearities on Statistical Distributions in the Theory of Sea Waves," *Journal of Fluid Mechanics*, Vol. 17, 1963, pp. 459-480.
29. Medina, J.R., "Estudio del Modelo Estadístico-Espectral del Oleaje y su Relación con las Técnicas de Simulación Numérica. Análisis Espectral y Estadístico de Registros," thesis presented to the Universidad Politécnica de Valencia, at Valencia, Spain, in 1982, in partial fulfillment of the requirements for the degree of Doctor.
30. Nagai, K., "Diffraction of the Irregular Sea Due to Breakwaters," *Coastal Engineering in Japan*, Vol. 15, 1972, pp. 59-67.

31. Phillips, O.M., "The Equilibrium Range in the Spectrum of Wind-generated Waves," *Journal of Fluid Mechanics*, Vol. 4, 1958, pp. 426-434.
32. Pierson, W.J., Jr., and Moskowitz, L., "A Proposed Spectral Form for Fully Developed Wind Seas Based on the Similarity Theory of S.A. Kitaigorodskii," *Journal of Geophysical Research*, Vol. 69, No. 24, Dec., 1964, pp. 5161-5190.
33. Rye, H., "The Stability of Some Currently Used Wave Parameters," *Coastal Engineering*, Vol. 1, No. 1, 1977, pp. 17-30.
34. Scott, J.R., "A Sea Spectrum for Model Tests and Long-Term Ship Prediction," *Journal of Ship Research*, Dec., 1965, pp. 145-152.
35. Shinozuka, M., "Simulation of Multivariate and Multidimensional Random Processes," *Journal of the Acoustical Society of America*, Vol. 49, No. 1, Part 2, Jan., 1971, pp. 357-367.
36. Tuah, H., and Hudspeth, R.T., "Comparisons of Numerical Random Sea Simulations," *Journal of the Waterway, Port, Coastal and Ocean Division*, ASCE, Vol. 108, No. WW4, Proc. Paper 17488, Nov., 1982, pp. 569-584.
37. Wittig, L.E., and Sinha, A.K., "Simulation of Multicorrelated Random Processes Using the FFT Algorithm," *Journal of the Acoustical Society of America*, Vol. 58, No. 3, Sep., 1975, pp. 630-634.
38. Zelen, M., and Severo, N.C., "Probability Functions," *Handbook of Mathematical Functions*, M. Abramowitz and I.A. Stegun, eds., Dover Publications, Inc., New York, N.Y., 1968, pp. 949-953.

APPENDIX II .- NOTATION

The following symbols are used in this paper :

| | |
|--------------------|--|
| A_m | = Complex valued fast Fourier transform (FFT) coefficient; |
| B | = backward shift operator; |
| c_m | = random variable chi square distributed with two degrees of freedom; $\chi^2(2)$; |
| d_m | = parameter related to wave frequency and time interval; |
| f_c | = cut-off frequency; |
| f_m | = frequency of the wave component; |
| f'_m, f'_{m+1} | = frequency limits of a band spectrum; |
| f_{max}, f_{min} | = maximum and minimum frequency limits; |
| f_p | = peak frequency |
| g | = gravitational constant; |
| h | = water depth; |
| H_{max} | = maximum wave height; |
| H_s | = significant wave height; |
| $H_{0.5}$ | = median wave height; |
| $H(f)$ | = frequency response function; |
| i | = $\sqrt{-1}$ = imaginary unit number; |
| J | = large integer, usually a large power of 2 or 10; |
| k | = summation index; |
| k_m | = magnitude of wave number; |
| L | = number of direction components for each frequency; |
| l | = summation index; |
| M | = number of wave components; |
| m | = frequency domain summation index; |
| m_j | = jth spectral moment; |
| N | = number of data points of the time series; |

n = time domain summation index;
 p = autoregressive order of the ARMA model;
 $p(\cdot)$ = probability density function;
 q = moving-average order of the ARMA model;
 R_m = amplitude of the wave component;
 $S_{\eta\eta}(f)$ = continuous one-sided ^{variance} power spectrum for water surface elevations;
 $S_{\eta'\eta'}(f)$ = continuous one-sided ^{variance} power spectrum for water surface vertical velocities;
 $S_{\eta''\eta''}(f)$ = continuous one-sided ^{variance} power spectrum for water surface vertical accelerations;
 $S_{\eta^{(k)}\eta^{(k)}}(f)$ = continuous one-sided ^{variance} power spectrum for water surface kth derivative of the elevation function;
 $S_{\eta\eta}(f, a)$ = continuous one-sided ^{variance} directional power spectrum for water surface elevations;
 \bar{T} = mean wave period of a realization;
 \bar{T}_0 = $\sqrt{m_0/m_2}$ = mean wave period parameter;
 u_m = rational pseudo random number between 0 and $\frac{J-1}{J}$;
 u'_m = integer pseudo random number between 0 and J-1;
 $u[\cdot, \cdot]$ = random number uniformly distributed in the interval between $[\cdot, \cdot]$;
 w_n = white noise time series;
 x, y = horizontal coordinates;
 z_n = onedimensional time series;
 Z_m = DFT(z_n), discrete Fourier transform of z_n ;
 a_θ = angle of directional component;
 a_0 = angle of reference direction;
 β_ε = coefficient;
 Δf = frequency interval;
 Δf_m = component interval;

Δt = time interval;
 Δa = angle interval of directional component;
 $\delta(f)$ = Dirac's delta function;
 ϵ = spectral bandwidth parameter;
 $\psi(B)$ = transfer function;
 ϕ_k = kth autoregressive parameter;
 θ_m = mth moving-average parameter;
 $\eta(t)$ = water surface elevation;
 θ_m = random phase angle;
 λ_1, λ_2 = integers between 0 and (J-1);
 π = 3.14159265...;
 $\sigma(\cdot)$ = standard deviation;
 $\chi^2(j)$ = chi square distribution with j degrees of freedom; and
 ω = $2\pi f$ = radian frequency.

Superscript

$*$ = complex conjugate value; and
 $' , '' , \dots , ^k$ = first, second, ..., kth derivative.

Subscript

$\eta\eta$ ^{variance} = power spectrum for water surface elevation, η ;
 $\eta^k\eta^k$ ^{variance} = power spectrum for kth derivative of water surface elevation, η^k ;
 j = jth moment;
 k = summation index;
 l = summation index;
 m = summation index; and
 n = summation index.

LIST OF CAPTIONS

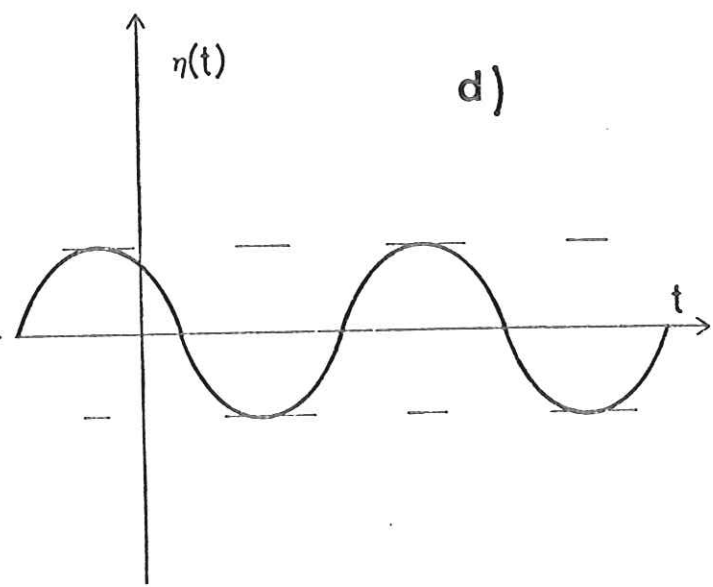
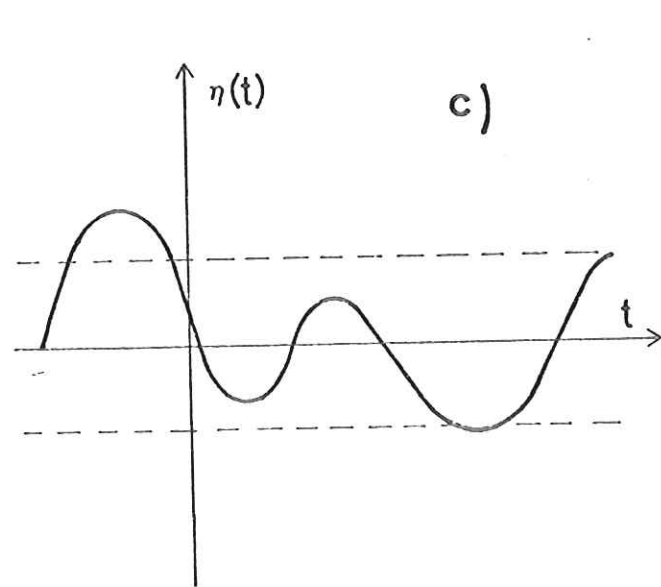
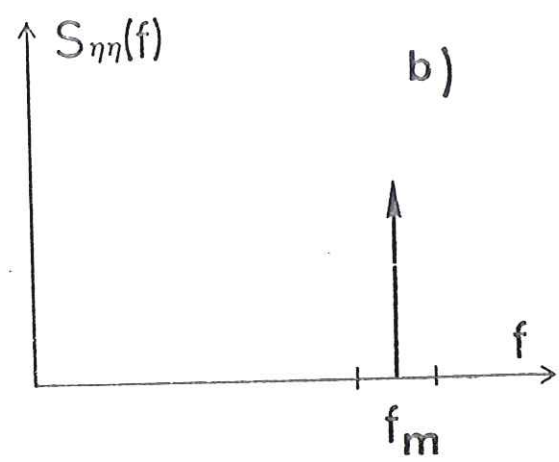
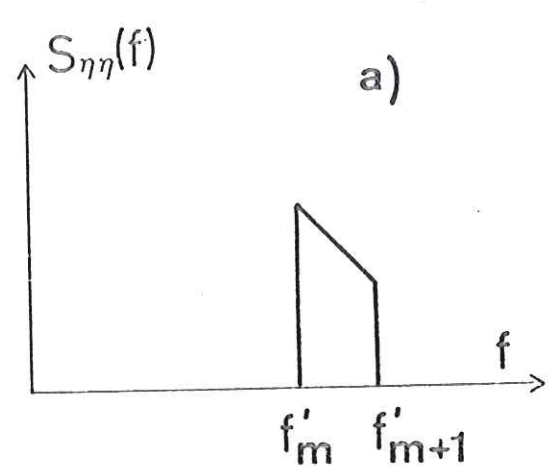
FIG. 1.- Schematic representation in the time and frequency domain of the change in the information about the band spectrum process to be simulated.

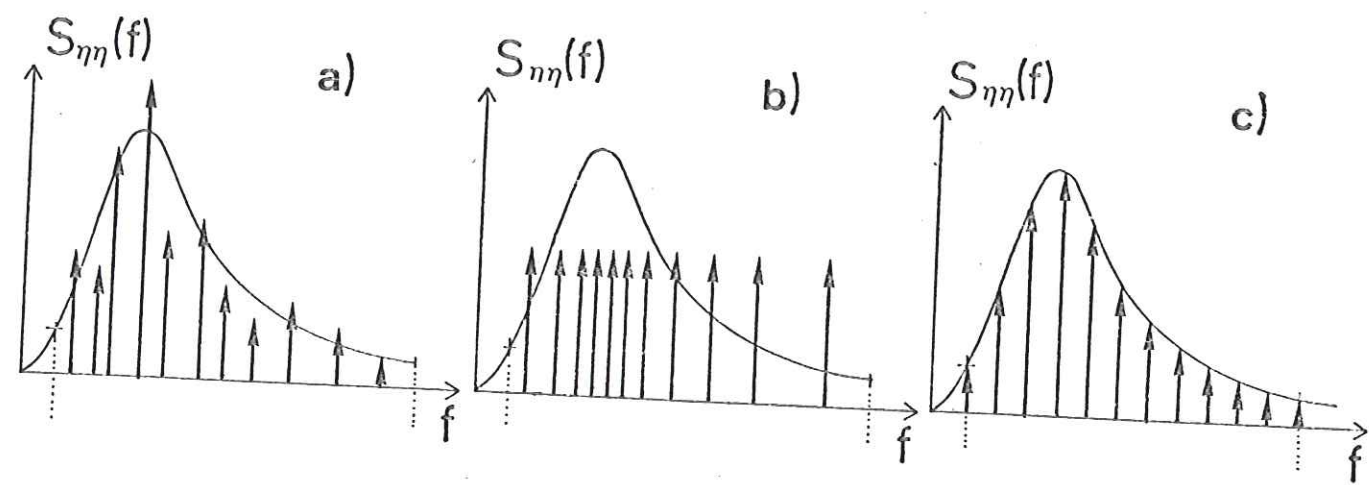
FIG. 2.- Schematic representation in the frequency domain of the Goda, Borgman, and DSA-FFT simulation techniques.

FIG. 3.- Relative spectral moments corresponding to B1,B2 and DSA simulation techniques referring to theoretical ones.

TABLE 1.- Influence of the cut-off-frequency on the parameters σ_{η}^2 , $\sigma_{\eta^2}^2$, $\sigma_{\eta^3}^2$, ϵ and \bar{T}_0 .

TABLE 2.- Mean and standard deviation estimates of relative wave statistics from sequences generated by different numerical random sea simulators.





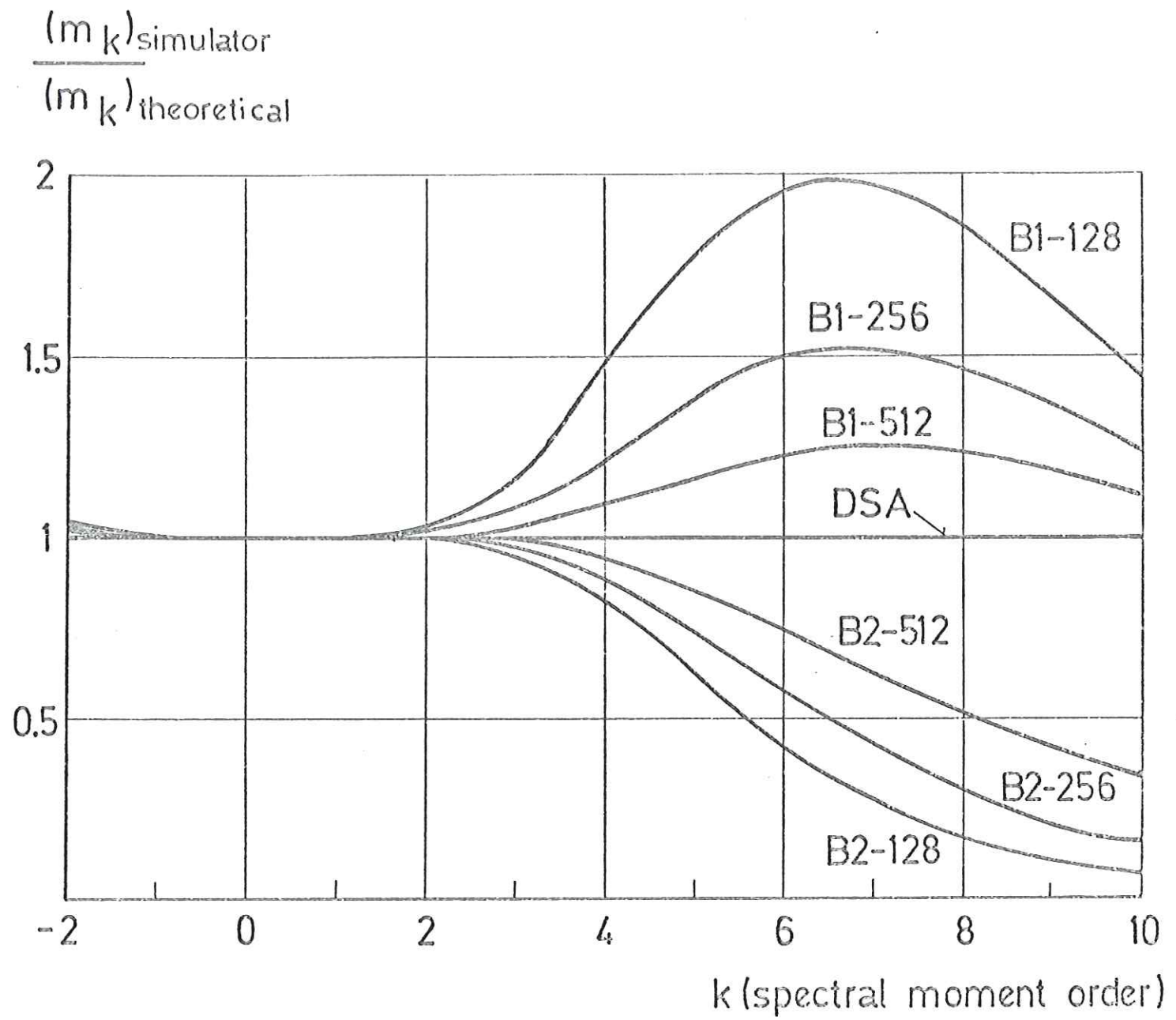


TABLE 1.--Influence of the cut-off frequency on the parameters σ_{η}^2 , $\sigma_{\eta'}^2$, $\sigma_{\eta''}^2$, ϵ and \bar{T}_o .

| | | | | | | | |
|--|-----|-------|-------|-------|-------|-------|-------|
| Cut-off frequency, in hertz | (1) | 0.200 | 0.333 | 0.400 | 0.500 | 1.000 | 4.000 |
| σ_{η}^2 , in square feet | (2) | 65.66 | 66.41 | 66.47 | 66.50 | 66.52 | 66.52 |
| $\sigma_{\eta'}^2$, in square feet per square second | (3) | 18.24 | 19.96 | 20.25 | 20.50 | 20.81 | 20.91 |
| $\sigma_{\eta''}^2$, in square feet per second ⁴ | (4) | 7.92 | 12.21 | 13.74 | 15.62 | 21.42 | 32.66 |
| ϵ | (5) | 0.600 | 0.713 | 0.742 | 0.772 | 0.834 | 0.895 |
| \bar{T}_o , in seconds | (6) | 11.92 | 11.46 | 11.38 | 11.32 | 11.23 | 11.21 |

Note: PMK spectrum, peak frequency $f_p = 0.0635$ Hz, zeroeth spectral moment $m_o = 66.5$ sq ft (6.19 m^2). $\bar{T}_o^p = (m_o/m_2)^{1/2}$

TABLE 2.-Mean and standard deviation estimates of relative wave statistics from sequences generated by different numerical random sea simulators.

| Simulator --- Number of components | rms elevations $\frac{z_{rms}}{(m_o)^{1/2}}$ | significant wave height $\frac{H_s}{4(m_o)^{1/2}}$ | mean wave height $\frac{H_{0.5}}{(8 \cdot \ln 2 \cdot m_o)^{1/2}}$ | mean wave period $\frac{\bar{T}}{(m_o/m_2)^{1/2}}$ | maximum wave height ^a $\frac{H_{max}}{(H_{max})_o}$ |
|---|---|--|--|--|--|
| (1) | (2) | (3) | (4) | (5) | (6) |
| ^b B1-64 | 1.007(0.046) | 0.965(0.044) | 0.995(0.118) | 1.021(0.063) | 0.896(0.099) |
| B2-64 | 1.006(0.046) | 0.956(0.045) | 0.963(0.130) | 0.967(0.065) | 0.890(0.102) |
| B1-128 | 0.997(0.064) | 0.951(0.069) | 0.985(0.113) | 1.017(0.060) | 0.888(0.102) |
| B2-128 | 0.997(0.065) | 0.953(0.067) | 0.972(0.092) | 0.995(0.050) | 0.895(0.104) |
| B1-256 | 0.995(0.074) | 0.955(0.079) | 0.975(0.110) | 1.017(0.056) | 0.905(0.099) |
| B2-256 | 0.993(0.074) | 0.951(0.079) | 0.977(0.114) | 0.999(0.058) | 0.906(0.111) |
| B1-512 | 1.006(0.082) | 0.964(0.086) | 0.977(0.107) | 1.021(0.054) | 0.907(0.140) |
| B2-512 | 1.005(0.082) | 0.964(0.087) | 0.978(0.119) | 1.014(0.064) | 0.900(0.142) |
| DSA-(256) | 1.000(0.000) | 0.954(0.019) | 0.985(0.094) | 1.017(0.061) | 0.926(0.078) |
| NSA-(256) | 1.022(0.072) | 0.979(0.074) | 1.014(0.106) | 1.034(0.063) | 0.949(0.136) |
| ^c B1-64 | 0.999(0.006) | 0.953(0.010) | 0.985(0.032) | 1.013(0.019) | 0.903(0.070) |
| B2-64 | 0.999(0.006) | 0.951(0.009) | 0.968(0.029) | 0.955(0.019) | 0.893(0.082) |
| B1-128 | 1.001(0.006) | 0.957(0.012) | 0.987(0.034) | 1.013(0.015) | 0.887(0.069) |
| B2-128 | 1.001(0.009) | 0.955(0.011) | 0.977(0.030) | 0.988(0.014) | 0.899(0.074) |
| B1-256 | 1.003(0.013) | 0.959(0.016) | 0.987(0.029) | 1.009(0.014) | 0.921(0.092) |
| B2-256 | 1.003(0.013) | 0.958(0.015) | 0.977(0.029) | 0.995(0.016) | 0.924(0.084) |
| B1-512 | 1.001(0.022) | 0.954(0.023) | 0.983(0.035) | 1.005(0.016) | 0.915(0.089) |
| B2-512 | 1.001(0.022) | 0.953(0.024) | 0.985(0.036) | 1.000(0.019) | 0.905(0.088) |
| DSA-(2048) | 1.000(0.000) | 0.955(0.008) | 0.985(0.029) | 1.006(0.015) | 0.921(0.073) |
| NSA-(2048) | 0.998(0.033) | 0.954(0.033) | 0.982(0.041) | 1.003(0.019) | 0.900(0.084) |

a The theoretical mean maximum wave height is $(H_{max})_o = (8m_o)^{1/2} \left[(\ln L_w)^{1/2} + \frac{0.57721566}{2(\ln L_w)^{1/2}} \right]$
 where $L_w = N \Delta t / (m_o/m_2)^{1/2}$

b Number of Data Points, N = 1024 (512 sec)

c Number of Data Points, N = 8192 (4096 sec)

Note: The theoretical sea spectrum is the same in all cases: PMK with peak frequency $f_p = 0.0635$ Hz, zeroth spectral moment $m_0 = 66.5$ sq ft, and cutoff frequency $f_c = 0.5$ Hz. Forty realizations have been made. Time interval $\Delta t = 0.5$ sec